

See discussions, stats, and author profiles for this publication at: <https://www.researchgate.net/publication/231171708>

# Correlation of Spectral Emission Intensity in the Inductively Coupled Plasma and Laser Induced Plasma During Laser Ablation of Solid Samples

ARTICLE in ANALYTICAL CHEMISTRY · JULY 1995

Impact Factor: 5.64 · DOI: 10.1021/ac00110a020

---

CITATIONS

32

---

READS

27

5 AUTHORS, INCLUDING:



**Alberto Fernandez**

Central University of Venezuela

66 PUBLICATIONS 889 CITATIONS

SEE PROFILE



**Xianglei Mao**

Lawrence Berkeley National Laboratory

167 PUBLICATIONS 4,682 CITATIONS

SEE PROFILE

# Correlation of Spectral Emission Intensity in the Inductively Coupled Plasma and Laser-Induced Plasma during Laser Ablation of Solid Samples

A. Fernandez,<sup>†</sup> X. L. Mao, W. T. Chan,<sup>‡</sup> M. A. Shannon,<sup>§</sup> and R. E. Russo\*

Lawrence Berkeley Laboratory, Berkeley, California 94720

Spectral atomic emission intensity from laser-induced plasmas (LIPs) exhibits excellent correlation with atomic emission intensity in the inductively coupled plasma (ICP) for a wide variety of materials and laser powers. Laser ablation sampling with introduction into an ICP for chemical analysis has, among other factors, a strong nonlinear dependence on laser energy, spot size, and material composition. The LIP emission also has a similar nonlinear dependence and is shown to correspond with the ICP behavior. The correlation is demonstrated for several homogeneous metallic and oxide materials during laser ablation sampling over a range of power densities and incident laser beam spot sizes. The correlation is best for higher melting temperature materials and moderate laser power density. The LIP and ICP emission intensities both show similar dependence for mass ablation rate versus power density and laser beam spot size. A normalized ICP/area over LIP emission ratio shows that a functional relationship can be found for changes in ICP intensity with changes in laser power density. The correlation shows that the ICP intensity accurately reflects changes in the laser ablation process and that the LIP may possibly be used for internal monitoring during laser sampling with the ICP.

Laser ablation sampling with inductively coupled plasma (ICP), atomic emission spectrometry (AES), mass spectrometry (MS), and microwave-induced plasmas (MIPs) offers important capabilities for chemical analysis of solid samples.<sup>1-7</sup> Direct analysis of

nonconducting and conducting samples, elimination of time-consuming sample preparation, localized microanalysis, and minimal personnel exposure are only some of the benefits that can be realized from laser ablation sampling. Many excellent papers have been published dealing with the advantages of laser ablation, and progress to date has advanced this technology to the commercial stage; several instrument companies offer laser ablation sampling attachments for ICP-AES and ICPMS. Comprehensive reviews of laser sampling for analytical chemical analysis were recently published by Moenke-Blankenburg<sup>1,2</sup> and Darke and Tyson.<sup>8</sup>

Analytical figures of merit (accuracy, precision, sensitivity) for laser ablation solid sampling can be similar to those obtained using solution nebulization for some samples. In addition, for laser ablation, the absolute quantity of sample can be 1  $\mu\text{g}$  or less, which is much lower than that required for dissolution and nebulization. There are several characteristics of laser ablation sampling that influence the quantity and chemical composition of the sampled material. Variations in the lasers' temporal and spatial profiles and power can contribute to nonlinear changes in ablation; the samples' physical and chemical matrix will effect the ablation behavior; and variations in the ablated particle size distribution can influence transport to the excitation source.

Averaging emission intensity from a number of laser pulses during a repetitive laser material interaction significantly improves precision.<sup>9,10</sup> However, this approach is not applicable to inhomogeneous samples or when localized microanalysis is desired. The use of materials with closely matched composition to the sample (standards) can be used to compensate for physical and chemical matrix effects, although the standards need to be exact replicas of the unknown to provide similar ablation and transport behavior. Precision can be improved slightly by monitoring the laser power, although the ablated quantity depends nonlinearly on power. Probably the most accurate method to determine mass removed is to weigh the target before and after laser sampling. However, such methodology is time consuming, cannot be performed in situ, exposes personnel to the sample, and has large relative uncertainty for very small mass removed (<1  $\mu\text{g}$ ).

Internal standardization has been widely used for laser ablation sampling.<sup>1,2,11,12</sup> This approach effectively compensates for varia-

\* Present address: Escuela de Quimica, Universidad Central de Venezuela, P.O. Box 47102, Caracas 1020-A Venezuela.

† Present address: Department of Chemistry, University of Hong Kong, Pokfulam Road, Hong Kong.

‡ Present address: Department of Mechanical Engineering, University of Illinois at Urbana-Champaign, Urbana, IL 61801.

§ Present address: Department of Mechanical Engineering, University of Illinois at Urbana-Champaign, Urbana, IL 61801.

(1) Moenke-Blankenburg, L. In *Laser Micro Analysis, A Series of Monographs on Analytical Chemistry and its Applications*; Wineforner, J. D., Kolthoff, I. M., Eds.; John Wiley & Sons: New York 1989; Vol. 105.

(2) Moenke-Blankenburg, L. *Spectrochim. Acta Rev.* **1993**, *15*, 1-37.

(3) Piepmeyer, E. H. In *Analytical Applications of Laser*; Piepmeyer, E. H., Ed.; Wiley: New York, 1986.

(4) Denoyer, E. R.; Fredeen, K. J.; Hager, J. W. *Anal. Chem.* **1991**, *63*, 445A-457A.

(5) van Haezen, A. A.; Morsink, J. B. W. *Spectrochim. Acta* **1991**, *46B*, 1819-1828.

(6) Uebbing, J.; Ciocan, A.; Neimax, K. *Spectrochim. Acta* **1992**, *47B*, 601-610.

(7) Moenke-Blankenburg, L. In *Laser Ionization Mass Analysis*; Vertes, A., Gribels, R., Adams, F., Eds.; John Wiley & Sons: New York, 1993; Chapter 4.

(8) Darke, S. A.; Tyson, J. F. J. *Anal. At. Spectrom.* **1993**, *8*, 145-209.

(9) Chan, W. T.; Russo, R. E. *Spectrochim. Acta* **1991**, *46B*, 1471-1486.

(10) Arrowsmith, P. *Anal. Chem.* **1987**, *59*, 1437-1444.

(11) Majidi, V.; Joseph, M. R. *Crit. Rev. Anal. Chem.* **1992**, *23*, 143-162.

(12) Quentmeier, A.; Sdorra, W.; Niemax, K. *Spectrochim. Acta* **1990**, *45B*, 537-546.

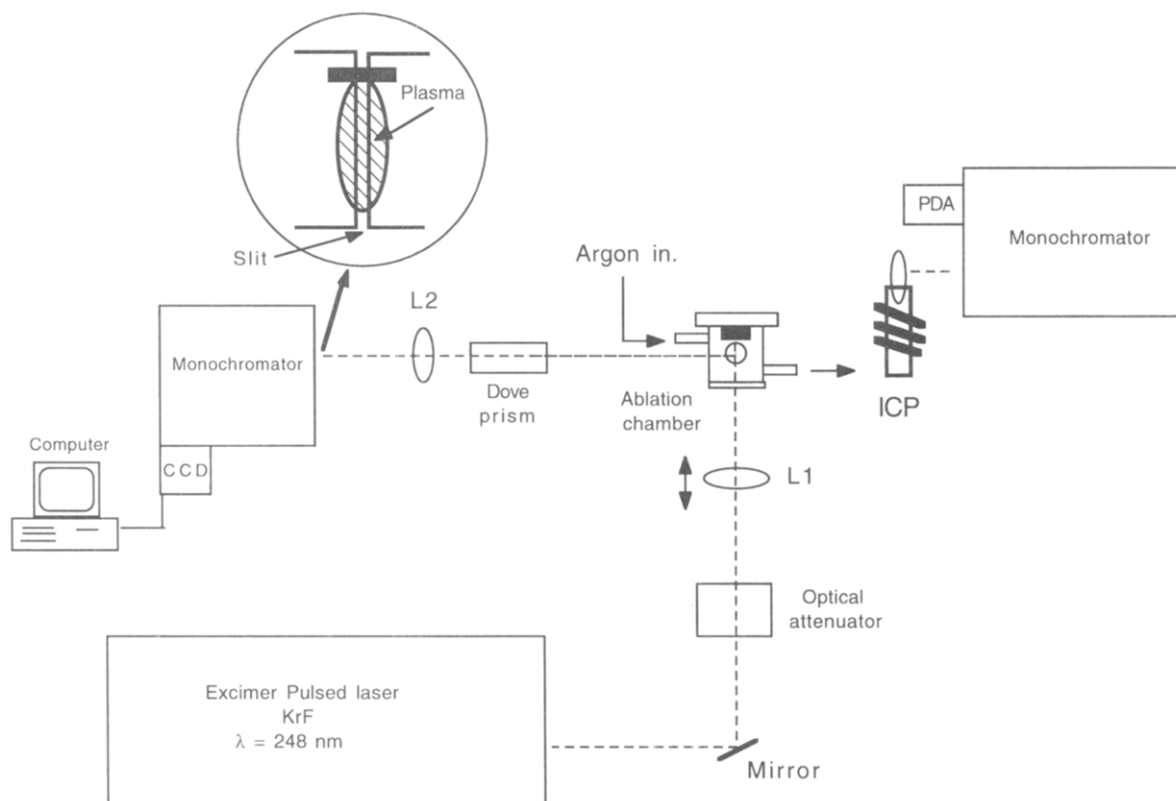


**Figure 1.** Diagram of experimental system for measuring emission intensity from laser-induced plasmas and from the inductively coupled plasma. Inset shows axial channel of plasma that is imaged by lens and CCD spectrometer for one experimental series. L1 and L2 are lenses.

tions in the analyte signal due to changes in the quantity of the ablated material. For this methodology though, the spatial distribution of the internal standard must be homogeneous. Also, the internal standard and the analyte must be equally affected by the laser material interaction. These premises are not always reliable, as preferential vaporization can occur. Because of these issues, several groups have investigated other technologies to improve laser ablation sampling. Acoustic response was demonstrated to be linearly related to the emission intensity in the laser-induced plasma.<sup>13</sup> Light scattering from the laser-ablated vapor in the sample cell was found to be related to ICP emission intensity.<sup>14</sup> A combination of solution nebulization and laser ablation sample introduction was studied for analyte quantification and improved precision.<sup>1,15</sup> Finally, a mass monitor was utilized to weigh a portion of the laser-ablated sample, to correct for variations in the ablated quantity and sample transport.<sup>16</sup>

In this paper, we demonstrate another approach in which elemental spectral emission intensity in the ICP is related to that measured in the laser-induced plasma (LIP). The correlation of spectral emission measured for the LIP and the ICP is investigated in terms of both understanding the laser material interaction and developing a potential methodology for normalizing ICP-AES measurements. This approach is demonstrated for several samples and over a wide range of laser power density. Spectral emission intensity from Cu, Al, and Zn is measured from Cu, brass,

Al, Zn, and  $\text{Al}_2\text{O}_3$  targets. The effect of laser beam irradiance and spot size on ICP and LIP emission intensity is investigated. These correlation studies demonstrate how the laser material interaction changes with irradiance and influences analytical measurements. The interaction between a pulsed laser beam and solid samples must be understood on a fundamental level so that optimum laser parameters can be selected a priori to achieve sensitive, accurate, and precise chemical analysis.

## EXPERIMENTAL SECTION

A diagram of the experimental system is shown in Figure 1. The beam from a KrF ( $\lambda = 248$  nm) pulsed excimer laser (Questec; 2860) is directed into the ablation sample chamber using a mirror and focused onto the sample surface using planoconvex UV-grade quartz lens ( $f = 20$  cm). The lens is mounted on a micrometer translation stage, so that the laser beam spot size at the target surface can be finely adjusted. The laser pulse duration is 30 ns, and the repetition rate is 5 Hz. A 6 mm diameter aperture is placed between the excimer laser and the focusing lens so that only the homogeneous central portion of the excimer laser beam is transmitted to the sample surface.

Samples are always placed before the effective focus of the lens to eliminate breakdown and plasma formation of the gas (Ar). Metallic Cu, brass, Al, Zn, and the insulator  $\text{Al}_2\text{O}_3$  are used as targets. These targets are 2 cm diameter and approximately 1 mm thickness. A flat, smooth surface of the sample is obtained by polishing with 400 mesh silicon carbide paper, although our experience indicates that this minor sample preparation is not necessary. The samples are not translated or rotated during each measurement. Instead, repetitive laser sampling at each spot digs a crater in these homogeneous materials and the emission

(13) Chen, G. Y.; Yeung, E. S. *Anal. Chem.* **1988**, *60*, 2258–2263.

(14) Richner, P.; Borer, M. W.; Brushwyler, K. R.; Hieftje, G. M. *Appl. Spectrosc.* **1990**, *44*, 1290–1296.

(15) Thompson, M.; Chernery, S.; Brett, L. J. *Anal. At. Spectrom.* **1990**, *5*, 49–55.

(16) Baldwin, D. P.; Zamzow, D. S.; D'Silva, A. P. *Anal. Chem.* **1994**, *66*, 1911–1917.

intensity from repetitive laser pulses is averaged.

A quartz sample chamber was constructed with the same geometry as described previously.<sup>9,17,18</sup> Gas flow through the chamber is regulated by a needle valve and measured using a mass flowmeter (Matheson; 8112-0423) at 1.00 L/min. The exit port of the ablation chamber is connected to the central channel of the ICP torch. The ICP (Plasma Therm; 2500D, 27 MHz) is operated at 1.25 kW forward power and 15 L/min outer Ar gas flow. Spectral emission from the ICP is imaged using a quartz lens (20 cm focal length) onto a 0.32 m monochromator (Instruments SA Inc.; HR-320) with a 1200 groove/mm grating and a slit width of 50  $\mu\text{m}$ . The detector is a thermoelectrically cooled photodiode array (PDA) (EG&G Par; 1412). The wavelength range dispersed simultaneously across the PDA is about 60 nm. The imaged region in the ICP is from 15 to 20 mm above the load coil.

The effects of laser beam spot size and power density on ablation behavior are investigated. Two procedures are used to change the laser power density. The first is to fix the spot size at 25, 100, 250, and 350  $\mu\text{m}$  and change the laser energy using an optical attenuator (Newport; 935-10). The second is to fix the laser energy and change the lens to target distance; the spot size of laser beam is changed. Power density at the sample surface is calculated from the energy of the laser beam, pulse width, and spot area. The spot area is calculated by use of geometric optical principles and compared to burn pattern measurements.

Two different experimental systems are used to measure emission from the laser-induced plasma. The first configuration images the central channel of the LIP, and the second images the entire LIP. The first LIP study involves the fixed laser beam spot sizes with variable laser energy to change the power density at the target surface. The LIP is imaged (1:1) via a camera lens and dove prism onto the entrance slit (12.5  $\mu\text{m}$ ) of a 0.27 m monochromator (Spex Industries; 270M, 1200 grooves/mm holographic grating). The central channel of the plasma, along its axis of expansion, is imaged onto the entrance slit of the monochromator (inset in Figure 1). The monochromator is equipped with a thermoelectrically cooled, charged-coupled device, CCD (EG&G PAR, OMA VISION). This spectrometer system simultaneously measures a 30 nm wavelength range.

The second LIP study uses fixed laser energy and varying laser beam spot sizes. A 0.5 m monochromator with a photomultiplier tube is used to monitor the entire laser-induced plasma. For this one, the LIP is imaged by a biconvex fused silica lens ( $f = 150$  mm) with a demagnification ratio of 6:1. The monochromator slit width is 400  $\mu\text{m}$ . The spatial extent of laser-induced plasmas in 1 atm Ar varies from about 1 mm to 2.5 mm, depending on the power density.<sup>19</sup> Using this demagnification ratio, the entire laser-induced plasma is imaged into the monochromator. The emission intensity is recorded using a digital oscilloscope (Tektronix DSA602A).

Spectral emission intensity from elements in the ICP and LIP are measured simultaneously. For all data reported in this paper, emission intensities are integrated for 10 s during repetitive ablation/sampling, after a 120 s preablation. Preablation involves

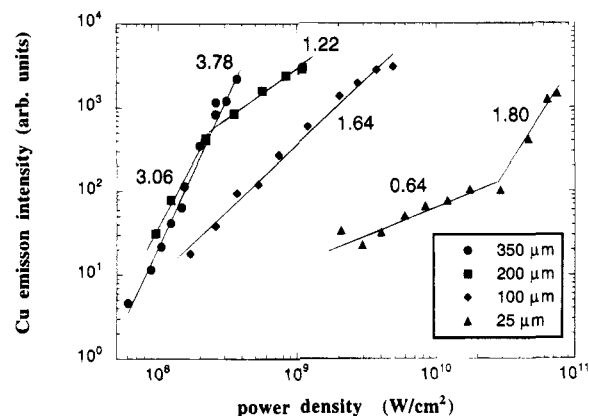


**Figure 2.** Cu emission intensity at 324.754 nm in the ICP as a function of laser power density. Laser energy and spot size are varied. Laser beam spot diameters are 350, 200, 100, and 25  $\mu\text{m}$ . Numbers represent the slope for change in mass removal versus power density.

repetitive pulsing at the sample location to “stabilize” the laser ablation/sampling response and improve precision.<sup>9,17,20</sup> The relative standard deviation (RSD) in emission intensity from the ICP during repetitive ablation/sampling is about 3%. By using an internal standard and repetitive pulsing, RSD can be improved to  $\leq 1\%$ .<sup>20</sup>

For measurements of the LIP using the CCD, data are corrected by subtracting the continuum emission measured on a both sides of each atomic emission line. The ICP emission intensity was corrected by subtracting the background emission obtained at the same wavelength without laser ablation sampling.

## RESULTS AND DISCUSSION

**Inductively Coupled Plasma Emission.** Spectral emission intensity in the ICP is related to the quantity of mass removed by laser ablation and the transport efficiency. Laser beam energy and spot size are important parameters influencing the ablation interaction, effecting the amount and composition of the sampled vapor.<sup>21</sup> An example is shown in Figure 2 for Cu emission at 324.754 nm in the ICP versus laser power density. These data show that emission intensity increases with laser energy at a different rate for four laser beam spot sizes (25, 100, 200, and 350  $\mu\text{m}$ ). The emission intensity  $I$  from the ICP is a function of laser power density,  $I = AP^m$ , where  $A$  is a constant,  $P$  is the power density, and  $m$  is the slope indicating the change in log of mass removal versus log of power density. The slopes were calculated by using linear fits to the data, with good correlation ( $r^2 > 0.99$ ) for all spot sizes. For the 100 and 350  $\mu\text{m}$  spot sizes, the intensity increases exponentially with the power density, although with different exponents; the exponent is almost double for the 350  $\mu\text{m}$  spot size. For the 200  $\mu\text{m}$  spot size, the emission intensity exhibits superlinear dependence (exponent  $> 1$ ) with power density up to 0.22 GW/cm<sup>2</sup>, above which the intensity increase at a much slower rate. For the smallest spot size of 25  $\mu\text{m}$  diameter, the emission intensity increases initially at a slow rate until above 40 GW/cm<sup>2</sup>, at which power density the emission intensity increases with a faster rate. The smaller to larger growth rates for the 25  $\mu\text{m}$  spot size represents contrasting behavior compared to the 200  $\mu\text{m}$  size, which goes from larger to smaller rates as laser energy is increased. However, the power density

(17) Chan, W. T.; Mao, X. L.; Russo, R. E. *Appl. Spectrosc.* **1992**, *46*, 1025–1031.

(18) Mao, X. L.; Chan, W. T.; Shannon, M. A.; Russo, R. E. *J. Appl. Phys.* **1993**, *74*, 4915–4922.

(19) Mao, X. L.; Shannon, M. A.; Fernandez, A. J.; Russo, R. E., submitted for publication in *Appl. Spectrosc.*

(20) Russo, R. E.; Chan, W.-T.; Bryant, M.; Kinard, J. *Anal. At. Spectrom.*, in press.

(21) Eyett, M.; Bauerle, D. *Appl. Phys. Lett.* **1987**, *51*, 2054–2055.

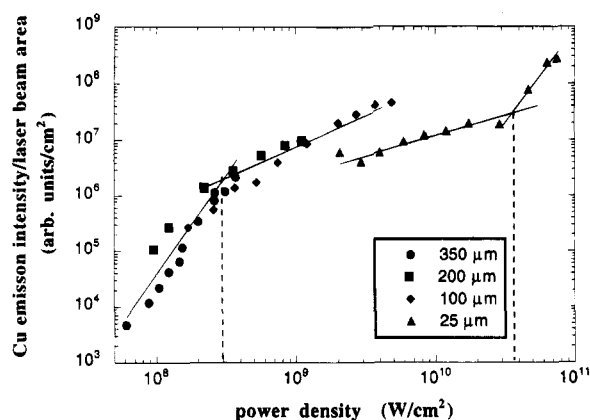


**Figure 3.** Cu emission intensity at 324.754 nm in the ICP normalized to the laser beam spot area as a function of laser power density.

regions are significantly different. From Figure 2, it is clear that the total mass removal rate and the corresponding ICP intensity are affected by both the laser energy and the incident laser beam spot size. The laser ablation mechanisms affecting material removal can change between different spot sizes, and even with the same spot size, as laser energy changes. A complete investigation of the dependence of the mass removal rates on laser spot size will be the subject of a future paper.

In order to investigate how changes in laser ablation influence material removal, the emission data are normalized to laser beam spot area on the target. Figure 3 shows the data for the four separate spot sizes when the ICP emission is normalized to laser beam area and graphed as a function of power density; three distinct ablation regimes are evident. The normalized ICP emission intensity is related to the number of atoms emitting per unit of projected area on the target, which gives an effective mass flux being removed from the target. The ICP intensity is assumed to be proportional to total ablated mass. With the mass ablation rate defined as the total mass ablated per unit time and area, the emission intensity divided by laser beam area is proportional to mass ablation rate. As seen in Figure 3, the mass ablation rate changes significantly when the power density exceeds approximately 0.25 GW/cm<sup>2</sup>, and again above 40 GW/cm<sup>2</sup>. For the 25 μm spot size, the data also show an offset in magnitude which may be due to the relatively deep craters produced during repetitive ablation, thereby changing the focal distance and power density. These data indicate a change in the ablation mechanism versus power density; the efficiency of energy coupling and sample removal is power density dependent. Similar behavior in data was measured when the energy of the laser beam was constant and the power density was increased by decreasing the spot size. The change in mass ablation rate may be due to a decrease of laser energy at the target surface and increased absorption, reflection, or both by surface plasma, a process known as plasma shielding.<sup>22</sup> We have observed similar ablation behavior for numerous samples, including metals, alloys, oxide insulators, and glasses.<sup>9,17,18,20</sup> In general, the mass ablation rate exponentially increases in the low-power density regime and drops to near unity or below at high-power densities. At still higher intensities, the ablation rate may increase again or drop further, depending on the spot size, material, gas medium, and laser wavelength and focus. An interesting observation is that the first roll-off of emission intensity

usually occurs at about 0.2–0.3 GW/cm<sup>2</sup> for conducting materials as well as some insulators, using UV nanosecond pulsed lasers. A complete discussion of the roll-off phenomenon is beyond the scope of this investigation and will be the subject of a subsequent paper.

A ramification of this behavior for ICP-AES and ICPMS is that the absolute mass sampled can vary significantly as the power density changes during a particular measurement or during averaging in a repetitive pulse case. As a crater develops, or for multiple analyses over an irregular surface, power density will change during the measurement. For homogeneous samples, the power density dependence can be minimized by measuring the ratio of the analyte to an internal standard.<sup>20</sup> This normalization requires that all elements respond similarly to changes in power density, which has been found to be the case for some glass samples but not alloys.<sup>9,20</sup> Also, the influence of power density changes can be minimized by operating in the power density regime >0.25 GW/cm<sup>2</sup> and <40 GW/cm<sup>2</sup>. In any case, it is desirable to know that changes in ICP-AES intensity are due to changes in analyte concentration and not the laser material interaction. Therefore, a normalization or real-time monitor of the laser material interaction is required.

**Laser-Induced Plasma Emission.** Laser-induced plasmas have been studied for many years as vaporization, atomization, and excitation sources for chemical analysis.<sup>23–27</sup> Their temporal and spatial emission behavior has been studied for fundamental understanding of the laser material interaction and to improve analytical capabilities. In this work, spectral emission intensity in the LIP is measured simultaneously with the emission intensity from the ICP for each particular element, as a means of studying changes in the ablation behavior and to normalize emission response changes in the ICP to changes in the laser material interaction. Time integrated, spatially resolved emission from the LIP using a 100 μm spot size and irradiance of 4.93 GW/cm<sup>2</sup> on a copper target is shown in Figure 4 (target is at position 0). Cu (I) emission is measured at 510.554, 515.334, 521.820, and 529.252 nm with a low continuum background (see Figure 4a). As seen in Figure 4b with the 521.82 nm line intensity normalized to the maximal intensity, the spectral emission intensities increase with distance from the target, reaching a maximum at approximately 1.5 mm and then decreasing as the distance from the target increases. The continuum emission spectrum followed similar behavior as the Cu emission. The spatial plasma emission strongly depends on the laser beam spot size and fluence, and on the integration time of the measurement.<sup>19</sup> For multicomponent samples, the measured spatial extent of plasma emission also depends on the particular species.<sup>28</sup> Plasmas from IR lasers have been reported to be more complex than those induced by UV lasers, because of laser–plasma interactions. Poor precision in LA ICPMS has been attributed to poor reproducibility in forming IR plasmas.<sup>29</sup> The UV laser-induced plasmas are believed to be more characteristic of the laser material interaction; our correlation

(22) Ready, J. F. *J. Appl. Phys.* **1965**, *36*, 462–468.

(23) Simeonsson, J. B.; Miziolek, A. W. *Appl. Phys. B* **1994**, *59*, 1–9.

(24) Majidi, V.; Rae, J. T.; Ratliff, J. *Anal. Chem.* **1991**, *63*, 1600–1602.

(25) Grant, K. J.; Paul, G. L. *Appl. Spectrosc.* **1990**, *44*, 1349–1354.

(26) Sdorra, W.; Niemax, K. *Spectrochim. Acta* **1990**, *45B*, 917–926.

(27) Radziemski, L. J.; Loree, T. R.; Cremers, D. A.; Hoffman, N. M. *Anal. Chem.* **1983**, *55*, 1246–1252.

(28) Lee, Y.-I.; Sawan, S. P.; Thiem, T. L.; Teng, Y.-Y.; Sneddon, J. *Appl. Spectrosc.* **1992**, *46*, 436–441.

(29) Geertsen, C.; Brian, A.; Chartier, F.; Lacour, J.-L.; Mauchien, P.; Sjöström, S.; Mermet, J. M. *J. Anal. At. Spectrom.* **1994**, *9*, 17–22.

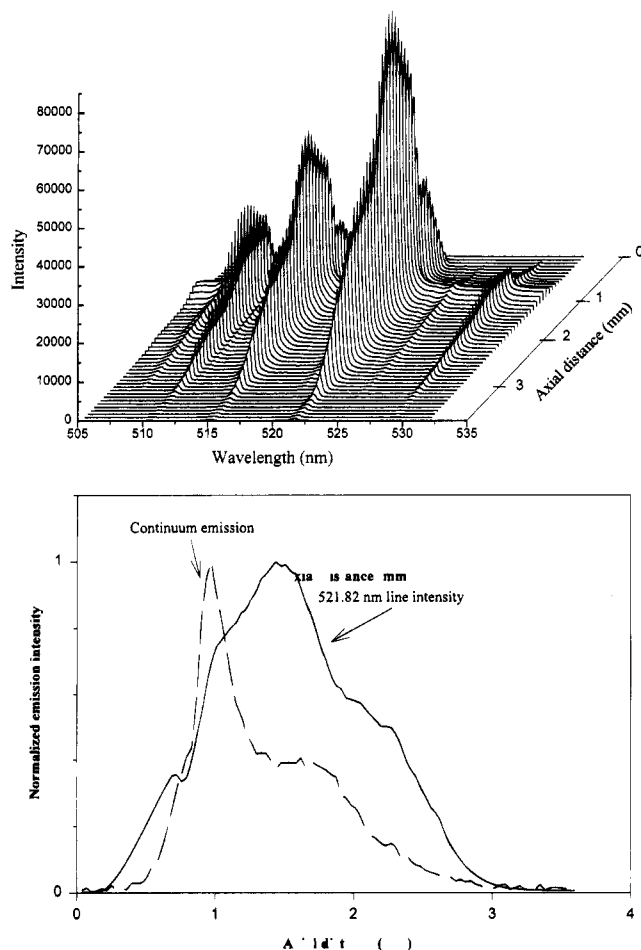


**Figure 4.** (a, top) Integrated Cu emission intensity versus axial position in the laser-induced plasma with laser power density of 4.93 GW/cm<sup>2</sup>. Target surface is at 0 axial position. (b, bottom) Emission intensity versus axial distance in the laser-induced plasma. The data are normalized to maximum intensity. The solid line is for Cu 521.82 nm emission intensity and the broken line is continuum background emission.

of ICP to LIP emission intensity is based on an UV-induced LIP.

Laser-induced plasmas exhibit complex spatial and temporal behavior. In the first few hundred nanoseconds, emission exists from ionic and neutral species. Emission from neutrals and molecular species can then last for several hundred microseconds. The time and spatial integrated measurements reported here only show the neutral emission lines. Line broadening and self-absorption have been reported for laser-induced plasmas, primarily during the first few hundred nanoseconds.<sup>30–32</sup> Broadening is related to self-absorption, which can cause self-reversal of resonance lines. If self-absorption occurs, it should be noticeable at the high-power density, and the full width at half-maximum (fwhm) of the emission line will change at the different axial positions, because of different plasma densities. The nonresonance emission lines selected in this work show the same line width at the different axial positions and the different power densities studied. Therefore, it is believed that self-absorption is negligible for the emission lines and the power densities used in this work.

**Emission Correlation.** Spatially and temporally integrated Cu (521.82 nm) emission intensity as a function of laser power

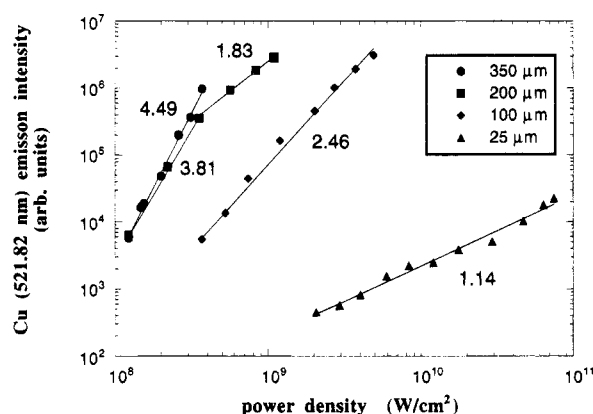


**Figure 5.** Cu emission intensity at 521.82 nm in the LIP as a function of laser power density. Laser beam spot diameters are 350, 200, 100, and 25 μm.

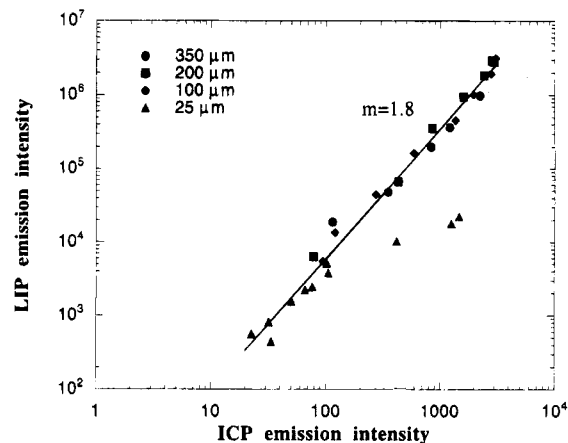


**Figure 6.** Correlation between Cu emission intensity in the LIP versus the ICP for the four spot sizes and power density range studied. The target is copper.

density from the 12.5 μm central channel of the LIP is shown in Figure 5 (for the same spot sizes and laser energy reported for the ICP in Figure 2). Similar to the emission measurements from the ICP, the LIP Cu emission intensity versus power density follows a power law dependence with exponent greater than 1. The exponent for the LIP Cu emission intensity using the 350 μm spot size is larger than that obtained for the 100 μm spot size. For the 200 μm spot size, two different exponents are measured, and the change is observed at approximately 0.30 GW/cm<sup>2</sup>, similar to the ICP behavior. For the smallest spot size of 25 μm, the LIP shows a constant increase with exponent slightly greater than unity. Cu emission in the LIP does not show a change in slope above 40 GW/cm<sup>2</sup> for the 25 μm spot size, as observed in the ICP because of the measurement configuration. Also, for the largest spot sizes at the lowest laser power, the sensitivity of the spectrometer system could not record the LIP emission intensity. Finally, the absolute values of the exponents are not expected to be the same for the ICP and LIP because they represent two different excitation sources, although they both depend on the number density or mass of laser-ablated sample. The ratio of data in Figure 5 to laser beam area was not calculated because only the central 12.5 μm channel of the plasma emission was measured. Normalization of LIP emission intensity is possible when the entire plume is imaged into the spectrometer. The curve in Figure 6 shows a good correlation between ICP and LIP emission intensities except the three data points which were obtained at power

(30) Austin, M.; Briand, A.; Mauchien, P.; Mermet, J. M. *Spectrochim. Acta* **1993**, *48B*, 851–862.

(31) Grant, K. J.; Paul, G. L.; O'Neil, J. A. *Appl. Spectrosc.* **1990**, *44*, 1711–1714.

(32) Grant, K. J.; Paul, G. L.; O'Neil, J. A. *Appl. Spectrosc.* **1991**, *45*, 701–705.

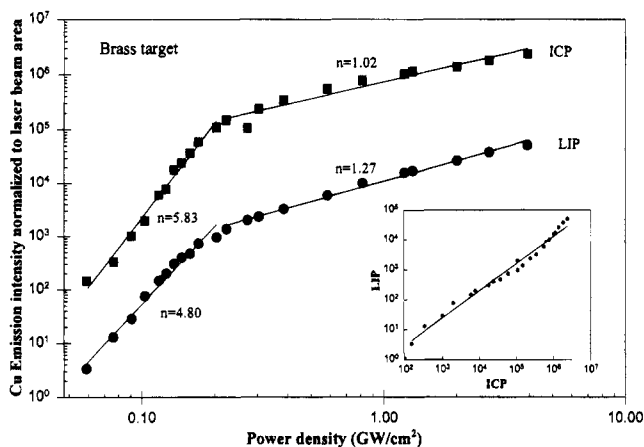


**Figure 7.** Cu emission intensity at 521.82 nm (normalized to laser beam area) in the LIP and ICP as a function of laser power density. The power density is changed by varying the laser beam spot size with fixed laser energy. Inset is the ratio of LIP to ICP intensities.

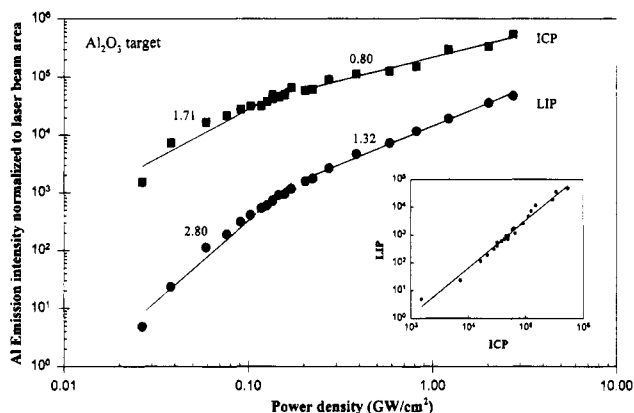


**Figure 8.** Al emission intensity at 396.15 nm (normalized to laser beam area) in the LIP and ICP as a function of laser power density. The power density is changed by varying laser beam spot size with fixed laser energy. Inset is the ratio of LIP to ICP intensities.

density higher than 40 GW/cm<sup>2</sup>. From the data in Figures 2, 5, and 6, it is clear that the ICP emission responds to changes in the laser ablation mechanism for the Cu target and the laser conditions used in this work. Therefore, for each laser beam spot size, variations in the ICP emission intensity with power density may be compensated by using a calibrated ICP versus LIP intensity curve (cf. Figure 6).

The ICP and LIP emission intensities versus power density were investigated using different targets: brass, aluminum, zinc, and the insulator aluminum oxide. The data in Figures 7–10 show LIP and ICP emission (normalized to area) as a function of the power density from the different samples. The inset in each figure is the correlation of LIP to ICP intensities. For these experiments, the entire LIP was imaged using the monochromator/PMT system. Therefore, elemental emission is integrated over the entire duration and spatial extent of the LIP. These data show similar behavior for the quantity of sample excited to emission in the LIP versus that reaching the ICP and the two distinct mass ablation regions. A good linear fit to the data is obtained except for zinc. The imprecision for the Zn samples may be due to large molten particles reaching the ICP because of the low melting points of this metal (see Table 1). The ICP emission intensity is proportional to total mass ablated if the particles are smaller than approximately 5  $\mu\text{m}$ .<sup>5,10</sup> However, the LIP emission

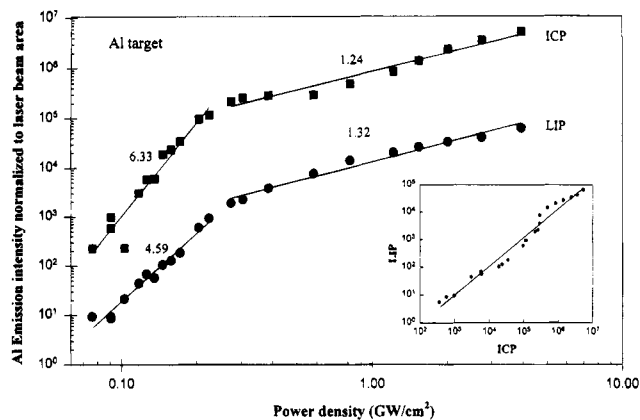


**Figure 9.** Al emission intensity at 396.15 nm (normalized to laser beam area) in the LIP and ICP as a function of laser power density. The power density is changed by varying laser beam spot size with fixed laser energy. Inset is the ratio of LIP to ICP intensities.

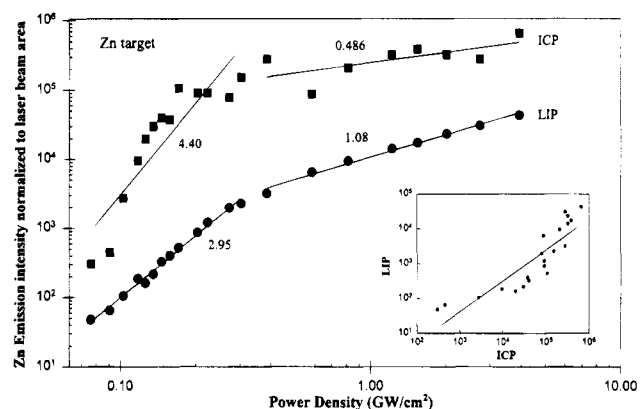


**Figure 10.** Zn emission intensity at 636.23 nm (normalized to laser beam area) in the LIP and ICP as a function of laser power density. The power density is changed by varying laser beam spot size with fixed laser energy. Inset is the ratio of LIP to ICP intensities.

**Table 1. Thermal Properties of the Elements and Rate Behavior from the Data in Figures 8–12**

	exponents <0.2 GW/cm <sup>2</sup>	exponents >0.2 GW/cm <sup>2</sup>	mp (°C)	bp (°C)
Cu in Cu	LIP > ICP	LIP ≥ ICP	1083	2595
Al in Al <sub>2</sub> O <sub>3</sub>	LIP > ICP	LIP > ICP	2045	2980
Cu in brass	ICP > LIP	LIP > ICP	915	
Al in Al	ICP > LIP	LIP ≥ ICP	660	2467
Zn in Zn	ICP > LIP	LIP > ICP	419	907

intensity will be proportional to total ablated mass vaporized, atomized, and excited, as well as the temperature of the plasma. If the number of atomic size particles is reduced in favor of larger melt ejecta, the LIP emission may be lower than the corresponding ICP intensity.

There is good correlation between ICP and LIP emission intensities for the higher melting point materials (such as brass and Al<sub>2</sub>O<sub>3</sub>). The correlation becomes noisy as materials with lower melting points are sampled (Al, Zn). The poor correlation for the Zn data may be due to the large dispersion measured for Zn emission in the ICP. The similar ICP and LIP emission intensities for Cu, Zn, brass, Al, and Al<sub>2</sub>O<sub>3</sub> indicate that the different mass removal rates originate from changes in the laser material interaction or ablation mechanisms and not due to changes in transport efficiency or in the average size of the ablated material versus power density.

Table 1 summarizes the mass ablation behavior for the different samples in the two distinct power density regions. In all cases, the exponents are greater for the LIP than ICP above 0.2 GW/cm<sup>2</sup>. A possible explanation for these data is that the plasma may limit the amount of laser energy transferred to the sample through plasma shielding. Laser energy absorbed by the LIP will increase the excitation temperature of the plasma providing the increase in emission intensity without an increase in the amount of ablated material. The LIP intensity is proportional to  $n \exp(-E/k_B T)$ , where  $n$  is density of atoms,  $E$  is energy level of a particular excitation, and  $T$  is excitation temperature. The ICP signal is related to the integration of density  $n$  whereas LIP emission is related to density  $n$  and the temperature  $T$ . A more complete discussion of measuring temperature in a LIP, and the effects of time integration on the LIP intensity in time and space, can be found in ref 19. In general, the LIP excitation temperature, and thus the population emitting at an energetic atomic line, increases as laser power density increases. Therefore, as the laser power density increases, the LIP intensity will increase unless the total mass of atoms substantially decreases. For the materials considered, and for most laser energy, wavelength, and spot sizes used, the LIP line emission intensity correlated with the ICP emission intensity, indicating that the mass contained in the laser-induced plasma corresponded with that removal rate during the laser ablation process. It should be noted that this may not always hold true, as seen in Figure 6 for power densities above 40 GW/cm<sup>2</sup>, for the smallest spot size.

We recently observed that the total LIP emission (spectral line and continuum background) monitored using a simple photodiode without a monochromator also exhibits similar intensity behavior versus laser power density. Such a system will be easier to incorporate as a normalization technique for ICP chemical analysis with laser ablation sampling.

## CONCLUSION

A direct correlation between inductively coupled plasma and laser-induced plasma atomic spectral emission intensities was

measured for different materials over a wide range of power densities. In addition, the correlation of ICP to LIP emission was observed in both cases, when only the central channel or the entire LIP was imaged. The observed correlation is important for two reasons. First, the good correlation to the LIP demonstrates that changes in ICP emission intensity appear to be primarily due to changes in the laser material interaction and not sample transport. If particle size distribution changes slightly versus power density, it may not influence the analysis as severely as the change in the interaction itself. Use of LIP emission to address transport and fundamental issues influencing ICP-AES requires more work to establish the effect of changing laser power density on the transport of analyte to the ICP. The second reason that the correlation is important is that it may be possible to use an LIP signal as a internal standard. From this work, it is apparent that over a large range of laser spot sizes and power densities that changes in the laser-material interaction during laser sampling may be accounted for through normalizing with the LIP signal, following calibration. Whether such an internal monitor of ICP spectral emission with LIP emission will ever be practical for routine analyses is as yet unknown. However, it is worth exploring a combination of the best aspects of each method: sensitivity, mass dependence, relative time independence with introduction into an ICP, and the inherent response of the LIP signal to the complex laser-material interaction occurring during laser sampling.

## ACKNOWLEDGMENT

This research was supported by the U.S. Department of Energy, Office of Basic Energy Sciences, Chemical Sciences Division, Processes & Techniques Branch, under Contract DE-AC03-76SF00098.

Received for review January 25, 1995. Accepted April 7, 1995.\*

AC950088C

---

\* Abstract published in *Advance ACS Abstracts*, June 15, 1995.